

Theses of Ph.D. Dissertation

**Structural study of the drug delivery systems and the kinetics of drug release**

Noémi Varga

Supervisor

Dr. Imre Dékány

Full professor, member of the Hungarian Academy of Sciences



Doctoral School of Chemistry

University of Szeged

Faculty of Science and Informatics

Department of Physical Chemistry and Material  
Science

Faculty of Medicine, Department of Medical Chemistry

Szeged, 2015

## 1. Introduction

The synthesis and precise characterization of the nanostructured materials and the nanocomposites and their application in practice made it one of the most intensively researched fields of modern colloid chemistry. Nanotechnology appears in more and more areas such as the environmental protection, agriculture, electronics, physics, informatics, pharmacy and nanomedicine. The simple synthesis, the favorable properties of the materials in nano-scale ( $\leq 100$  nm) contributed to the growth of nanotechnology. The key properties of these materials are the high surface area, the small size, the easy functionalization and the possibility of the conjugation with other molecules. The use of nanostructured materials provides opportunity to map the mechanism of the biochemical processes, to develop therapeutic applications, to explore what causes certain diseases and to treat those (medical diagnostics) and to rebuild cells.

In addition to the changes in the characteristics, the targeted specificity and the increased permeability through the membranes made nanoparticles attractive for application as drug delivery system. The application of numerous therapeutic agents in body is limited since their properties (like the structure, size, hydrophilic character, charge, solubility, stability, etc) prevent the targeted delivery and binding. Furthermore, the efficiency of the drug molecules may inhibit enzymatic cleavage or accumulation in a non-specific adsorption site. These barriers can be avoided by modifications, interactions with other molecules or application of transporters or composites. The disadvantage of the nanoparticles is their toxicity; the smaller the nanoparticle the more harmful it is for the body. For example, while Au nanoparticles have high toxicity below 15 nm, Ag and the  $\text{TiO}_2$  nanoparticles have same toxicity below 100 nm. Further disadvantage is that they could accumulate in the body while it does not have any function which can eliminate these substances. The solution for these problems will be the application of bioconjugates or composites, especially core-shell nanoparticles. Their advantages compared to the nanoparticles is their better biocompatibility: increased bio, and cytocompatibility, they have high level of dispersity and better conjugation with other bioactive molecules, improved thermal- and chemical stability. The role of the outermost shell which encapsulates the drug-containing carrier does not only prevent the toxicity, it can also increase the hydrophilic character of the system, it can stabilize the composite, it can improve the targeted delivery and it can execute a well-controlled drug release process. The ideal drug carrier systems are below 100 nm in size and they have high stability in the blood which

prevents the excretion of the active agents before the bioavailability. The most important criteria are that the controlled drug release should happen at the desired place in the appropriate time interval and in the adequate concentration. These requirements are essential since while small amount of a drug can be effective, a higher dosage of the same drug released in a short period of time could be harmful to the human body. Therefore, the preparation of the appropriate nanostructured materials and the study of their biological activity are complex tasks which involve discipline.

The aim of this research is to develop drug delivery systems which ensure sustained and controlled drug release under physiological conditions. The primary concern of the design of the carrier system was the application of biocompatible and non-toxic materials. The exclusion of the accumulation of the composites in the body was performed by making secondary binding forces between the components. A non-steroid inflammatory drug, the ibuprofen (IBU) and a central nervous system active agent, the kynurenic acid (KYNA) were chosen for encapsulation experiments. Accordingly, the aim of this work was to produce and characterize the following systems:

- a.) Synthesis and characterization of mesoporous silica ( $\text{SiO}_2$ ) for targeting of drug molecules.
- b.) Comprehensive physical-chemical investigation of the structure of the bovine serum albumin (BSA) between  $\text{pH} = 2$  and  $12$  in the function of  $\text{pH}$  in the absence and presence of  $150 \text{ mM NaCl}$  solution
- c.) Development of new-types drug delivery systems:
  - Two polyelectrolyte-layered  $\text{SiO}_2$ -based core-shell composites for encapsulation of IBU molecules.
  - Two polyelectrolyte-layered BSA-based core-shell composites for targeting of IBU molecules.
  - One-layered BSA-based core-shell nanocomposites for transporting KYNA molecules through the blood-brain barrier.
  - BSA/surfactant (sodium dodecyl sulphonate) complexes for the encapsulation of the IBU molecules.
- d.) Investigation of the mechanism of the release process of the prepared systems with empirical and mechanistic kinetic models.

### 3. Experimental materials and methods

#### 3.1. Experimental materials

3.1.1. Mesoporous silica ( $\text{SiO}_2$ ) particles were synthesized by the hydrolysis of tetraethyl-ortosilicate (TEOS) with application of a structure directing agent, the cethyl-trimethyl-ammonium-bromide (CTAB). The product was obtained by centrifugation (Hermle Z36HK) and calcinations process ( $550\text{ }^\circ\text{C}$ ) was used to remove the template.

3.1.2. During the preparation of the  $\text{SiO}_2$ -based core-shell composites the  $\text{SiO}_2$ /IBU composites were encapsulated by two oppositely charged polyelectrolytes, the polyethylenimine (PEI) and the poly(sodium-4-styrene sulphonate) (PSS) via electrostatically interactions after the formation of the interactions between the ibuprofen (IBU) and the silica particles ( $\text{pH} = 5.5$ ).

3.1.3. The bovine serum albumin (BSA) was chosen as the carrier in the core-shell particles. For the physical-chemical investigations of the BSA conformation, 3 mg/ml BSA solutions were prepared between  $\text{pH} = 2$  and 12 in the absence and presence of salt.

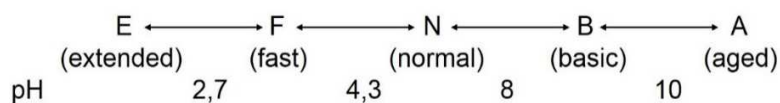


Fig.1. The conformational states of the proteins in the function of pH

3.1.4. During the formation of the BSA-ligand interactions the BSA concentration was kept at constant values and the hydrophobic ketoprofen (KP) or the 8-anilino-naphtalene sulphonic acid (ANS) molecules were added to the BSA-solution or to the BSA/KP complex ( $n_{\text{BSA}}:n_{\text{KP}}=1:1$ ) in increasing molar ratio (1: 0- 10).

3.1.5. The preparation of the two-layered BSA-based core-shell composites was carried out by the precipitation of the BSA/IBU composites at  $\text{pH} = 3$  buffer solution (McIlvaine-buffer). The composites were encapsulated by the negatively charged PSS (3 mg/ml) and the positively charged polysaccharide, the chitosan (Chit) (3 mg/ml).

3.1.6. For the preparation of the one-layered core-shell nanocomposites, kynurenic acid was bound to the protein in 1: 0.5 weight ratio at  $\text{pH} = 7.4$ , then the composites were encapsulated by poly(allylamine hydrochloride) (PAH) in 2.4 mg/ml concentration.

3.1.7. The BSA/SDS complexes were synthesized according to the following protocol: anionic surfactant (sodium dodecyl sulphate (NaDS)) was added in increasing concentration (0 – 6.3 mg/ml) to the BSA solution (5 mg/ml) at pH = 3.

3.1.8. For the preparation of the IBU-containing bioconjugates the concentration of BSA (5 mg/ml), the surfactant (6.3 mg/ml) and the NaCl (150 mM) were kept at a constant concentration and the IBU was added to BSA/NaDS complexes in increasing concentration (0 – 2 mg/ml).

### 3.2. *Experimental methods*

The surface area and the pores distribution of the silica particles were determined by using nitrogen adsorption/desorption methods (Micromeritics Gemini 2375, 77K).

Charge titrations were used to determine the charge compensation point by Mütéc PCD-04 particle charge detector.

The molecular weight of the protein, the average diameter and the zeta potential of particles and the composites were determined by light scattering method (Horiba SZ-100).

The size and the shape of the composites were characterized by transmission electron microscopy (TEM, FEI Tecnai G2 20 X-Twin) method.

In the BSA-containing samples, fluorescence methods were used by using Horiba Yvon Fluoromax-4 type apparatus ( $\lambda_{\text{ex}} = 280 \text{ nm}$ ).

The density and the thermoanalytical methods were carried out by a DMA 50 (Anton Paar) type densimeter, as well as Mettler Toledo TGA/SDTA 841e and Mettler Toledo 822<sup>e</sup> type apparatus.

The formation of the core-shell composites and the changes in the protein structure were followed by infrared (FT-IR, Biorad FTS-60A, ATR) and circular dichroism (CD, Jasco-815) spectroscopy.

XRD (Bruker D8) and SAXS (Philips PW 1820) measurements were used to study the structure of the samples.

The in vitro drug release experiments were carried out with the application of Hanson-cell and were followed by UV-vis detection.

Lyophilizer apparatus (Christ-Alpha 1-2 LD) was used to rapid freeze the BSA as well as to preserve the samples.

## 4. New Scientific Research

### 4.1. Structure of the SiO<sub>2</sub>-based core-shell composites and the kinetics of the drug release

4.1.1. It has been observed that the silica particles ( $d = 408$  nm) with  $1250$  m<sup>2</sup>/g surface area and  $3.3$  nm average pore diameter are able to bind  $\sim 1600$  mg/g IBU molecules. The ordered hexagonal mesoporous structure of the silica particles were proven by SAXS measurements. The continuously increasing fractal dimension values proved that the IBU diffuses into the pores ( $a = 2 - 2.75$ ) as well as the shells are formed around the SiO<sub>2</sub>/IBU composites. The formation of the interaction between the components was confirmed by FT-IR spectroscopy with the appearance of the characteristic peaks in the infrared spectra. [2]

4.1.2. Knowledge of the concentrations, the density (core and shell) and the diameter ( $408$  nm) of the SiO<sub>2</sub> particles, the shell thickness and the diameters of the one-layered core-shell composite were determined. The measured and the calculated diameters showed good agreement; the standard deviation of the spherical core-shell model is within  $10\%$  while of the core-shell model knowledge of the densities is  $8.9\%$ . The core-shell model knowledge of the concentration of the core given perfect match to the measured value (standard deviation is within  $\pm 1\%$ ). Therefore, using the suggested equations is a useful method to determine the expected diameter knowledge of the concentrations and the densities.

4.1.3. Based on the drug release experiments, the released amount of IBU was significantly reduced by increasing the number of the shells: during the  $500$  min test time the percent of the dissolved drug decreased by  $40\%$  in the two-layered core-shell composites compared to the SiO<sub>2</sub> particles. For the quantitative description of the release mechanism for the SiO<sub>2</sub>/IBU composites the zero-order (independent from the drug concentration) while for the SiO<sub>2</sub>/IBU/PEI core-shell composites the first-order rate model is applicable. The release process was controlled by erosion and diffusion from the SiO<sub>2</sub>/IBU/PEI/PSS core-shell composites. The  $k_d$  values continuously decrease with increasing the number of the shells which values for the SiO<sub>2</sub>/IBU; SiO<sub>2</sub>/IBU/PEI and the SiO<sub>2</sub>/IBU/PEI/PSS composites, without carrier,  $1.7 \cdot 10^{-3} \text{ s}^{-1}$ ; as well as for the composites are  $2.5 \cdot 10^{-3} \text{ s}^{-1}$ ;  $1.0 \cdot 10^{-3} \text{ s}^{-1}$  and  $6.0 \cdot 10^{-4} \text{ s}^{-1}$ , respectively. [2]

## **4.2. Results of physical-chemical examination methods concerning the secondary and tertiary structures of BSA in the function of pH as well as in physiological salt solution**

**4.2.1.** The changes in the BSA secondary structure were verified by FT-IR spectroscopy in the function of pH in physiological solution. The BSA in N-form contains the highest  $\alpha$ -helical content (~62% in the absence of salt, ~51% in 150 mM NaCl-solution) which structure occurs in smaller ratio by decreasing the pH (F,- E-form). In B- and A-forms the BSA has from 40 to 55%  $\alpha$ -helix content, depending on the pH and the presence of the salt. E- and F-form, which have the lowest  $\alpha$ -helix content, contain the highest amount of aggregated structure, around 12%, while N-form contains only around 2.5% aggregated structure. [4]

**4.2.2.** The tertiary structure of the BSA was characterized by fluorescence measurements. The protein in native, i.e. in folded-state has the highest emission peak, while in the case of flatter peak with lower intensity confirmed the appearance of the unfolded protein. The structural rearrangement is higher in alkaline pH range (there are well hydrated carboxyl groups on the surface) than in acidic media (there are non-polar and weak hydrated amino acids on the surface). [4]

**4.2.3.** It has been proven that the physiological solution caused the aggregation of the BSA protein which was verified by the increase in the hydrodynamic diameter (approximately doubled). Near the isoelectric point (pH = 5) the salt does not influence the size of the folded protein, the average diameter is 6 nm. The size of the unfolded protein is higher compared to the size of the protein in native form which was supported by SAXS measurements (at pH = 3 is  $D = 9$  nm; at pH = 7.4 is  $D = 6.3$  nm). The protein has high stability in alkaline pH range ( $\zeta = -28$  mV – - 69 mV), however electric double layer was formed in the presence of NaCl-solution ( $\zeta = -0.9$  – -2.4 mM) which has led to the aggregation of the protein. [4]

**4.2.4.** Based on the results of the static light scattering it can be stated that the BSA is mainly in monomer form at pH = 3 (54.6 kDa), at pH = 7 (65.3 kDa) and at pH = 11 (68.6 kDa). The second virial coefficient helps concluding that the protein is in a well-solvated form at all pH in the absence of salt. Higher  $M_w$  values were measured in the presence of salt. Therefore, at pH = 3 (114

kDa) mainly dimer form was developed with association of two protein molecules. The  $M_w$  values are 78 and 83 kDa at pH = 7 and 11, respectively, which indicates that the protein contains the dimer form in increased ratio. At the last two pH values (pH = 7, 11) the negative values of the  $A_2$  indicate aggregation which is supported by the measured molecular values. [4] The equivalent radius is definable from the calculated molecular volume in the knowledge of the  $M_w$ , which values are similar to those obtained by DLS measurements. It can be proven based on the results of the geometric volume that the BSA in native-form has a spherical structure, while at acidic (pH = 3) or alkaline (pH = 11) pH range the geometry of the BSA can be describe with an extended, ellipsoid shape. [4]

### **4.3. Structure of the BSA-based two-layered core-shell composites and the kinetic of the drug release**

**4.3.1.** Increased solubility (60-fold) was achieved by the binding the IBU molecules to the BSA protein (pH = 3). [1]

**4.3.2.** In the unfolded protein structure, at pH = 3 the largest percent of the secondary structure unit is the  $\beta$ -sheet which was verified by the appearance of the amid I peak at  $1642\text{ cm}^{-1}$  wavenumber (FT-IR). The binding of the drug molecules caused structural changes in the BSA structure, i.e. a significant fraction of the protein became random coil (maximum of the amid I peak is  $1648\text{ cm}^{-1}$ ). The structure of the BSA becomes ordered due to the effect of the negatively charged PSS which was proven by the shifting of the amid I peak toward to the lower wavenumbers ( $1639\text{ cm}^{-1}$ ). The chains of the BSA, which is the carrier of the two-layered core-shell composites, unfolded again ( $1648\text{ cm}^{-1}$ ) by the effect of the branched, positively charged PEI. The chain-like structure in the case of the BSA/IBU composite was proven by SAXS measurements. In the case of the BSA and BSA/IBU composites individual scattering centers were recognized while for the one- and two-layered core-shell composites the presence of aggregates was confirmed. The pair distribution functions resulted in more and more widener and flatter curves by the formation of the composites which refers to a structural change in the BSA structure, namely the spherical structure became increasingly ellipsoid shape. [1]



**4.3.3.** The diameter of the one-layered core-shell composites is 130 nm ( $d_{TEM} = 138 \pm 18.0$  nm,  $d_{DLS} = 134 \pm 12.3$  nm; the BSA/IBU/PSS/Chit:  $d_{TEM} = 223 \pm 18.5$  nm;  $d_{DLS} = 231 \pm 9.6$  nm) which value implied that none of the BSA molecules was encapsulated by the PSS shell in 130 nm thickness. It was found that the core-shell model taking the densities into account describes perfectly (the calculated diameter is 130 nm) the measured diameter with the changing of the shell

thickness based on this equation:  $r_{Mag} = \left( \frac{d_{H\acute{e}j}^3 \rho_{H\acute{e}j} m_{Mag}}{\rho_{Mag} m_{H\acute{e}j}} \right)^{1/3}$ .

**4.3.4.** The release of the drug is initiated by changing the pH: the structure of the composite became loose as the result of the changed value of surface charge of the BSA (pH = 3:  $\zeta = +2.5$  mV, pH = 7.4:  $\zeta = -1.1$  mV). The two polyelectrolyte layers decreased the rate of the release by 40% after 500 min. The temperature did not have an influence on the released amount of IBU (~70%) in the case of the BSA/IBU composites. The release mechanism of the IBU from the BSA/IBU/PSS/Chit composites is erosion,- and diffusion-controlled at 25°C while at physiological conditions, i.e. at 37.5°C the release kinetic follows the zero-order rate model, i.e. a well-controlled release mechanism occurred (the release rate is independent from its concentration. [1]

#### **4.4. Structure of the one-layered core-shell nanocomposites and the kinetic of the drug release**

The KYNA, according to the stability studies, is stable in aqueous media at pH = 7 while in the presence of buffer (PBS, HEPES) the concentrations that have been measured for 24 hours differ from each other. Being aware of it, the preparation of the composites was carried out in physiological condition without buffer. [5,6] By investigating the fluorescence measurements of the BSA-ligand interactions it was found that the binding of ligand with carboxyl group to the BSA associated with high affinity and large free Gibbs energy ( $\Delta G$ ) at pH = 7.4.

**4.4.1.** Interactions between the polyelectrolyte and the BSA were weak while in the presence of drug molecules (500 mg KYNA / g BSA) strong interactions are formed between the KYNA and the PAH (for examples hydrogen-bridge, hydrophobic interactions) which were supported by DLS measurements: the size of the BSA/PAH composites is  $20 \pm 1.2$  nm while the diameter of the BSA/KYNA/PAH one-layered nanocomposites is 103 nm ( $d = 103 \pm 4.8$  nm). The formation of

the PAH layer around the BSA/KYNA composites was confirmed by the decrease in the Trp emission intensity. [5,6]

**4.4.2.** The BSA has 53.3%  $\alpha$ -helical content which is slightly decreased by being bound to the KYNA (51.8%) based on the CD spectra. The polyelectrolyte caused significant change in the protein structure: the content of the main secondary structure unit of the BSA is decreased to 29.6%. The PAH caused significant perturbation in the structure of the BSA during the formation of the KYNA-containing one-layered core-shell composites: the  $\alpha$ -helical content significantly decreased (15.9%) which is confirmed by DLS measurements. [5,6]

**4.4.3.** The KYNA was found stable in PBS-buffer only in the first hour is, therefore the kinetic models are applicable in this time period. The release mechanism from the BSA/KYNA composites was controlled by the diffusion at 25 and 37.5°C. In the case of the BSA/KYNA/PAH one-layered core-shell nanocomposites the zero-order rate model show the best fit which indicates that a constant KYNA concentration can be maintained in the given time period at physiological condition. [5,6]

#### **4.5. Structure of the BSA/IBU/NaDS composites and the kinetic of the drug release**

**4.5.1.** The necessary surfactant concentration needed to form a stable hydrophilic system for the transporting of IBU molecules was determined by preparing BSA/NaDS complexes with different molar ratio at pH=3:  $c_{BSA} = 5$  mg/ml and  $c_{NaDS} = 6.3$  mg/ml (1260 mg NaDS / g BSA). [3]

**4.5.2.** The liquid crystal structure of the surfactant was proven by the determination of the distance between the lamellas ( $d_L = 3.69$  nm). Taking the hydration state into account, the calculated  $d_L$  value was 3.97 nm which was in perfect agreement with the  $d_L$  value obtained by XRD measurements. The liquid crystal structure remained in the IBU/NaDS system; the distance values acquired for the NaDS are close to the  $d_L$  values (3.84 nm). The BSA caused partial disorientation in the liquid crystal structure; the decreased  $d_L$  distance (3.62 nm) suggests the sliding of the alkyl chains due to the effect of the protein. The well-defined (smectic) structure remained in the BSA/IBU/NaDS system owing to the drug molecules; by increasing the concentration of the IBU the  $d_L$  values received were in good agreement with the measured values for the NaDS. [3]

**4.5.3.** The ordered structure of the complexes was proven by SAXS measurements. The higher the concentration of the drug molecules is, the higher the intensities of the two peaks appeared in the scattering curves are at the IBU-containing composites (220 mg IBU / g BSA; 400 mg IBU / g BSA). It was recognized that the IBU ensures the stability of the liquid crystal (smectic) structure. The BSA is supposed to be the carrier in the system: the protein forms interactions with the alkyl chains of the surfactant with its hydrophobic parts while the polar head groups linked together form a lamellar structure. The IBU is probably located between the head groups and is bound to the protein. [3]

**4.5.4.** In the case of the release experiments, the surfactant significantly slowed down the release amount of IBU after 500 min time interval, the amount of dissolved IBU was only 17%. The percent of the released IBU is equal for both BSA/IBU and c11-BSA/IBU/NaDS composites (67%). A compact, well-ordered structure was formed by the increased concentration of the IBU which resulted in a low drug release percent (28%). Different models fit for the kinetics of the release of the IBU depending on the drug concentration; therefore for composites containing IBU in lower concentration the first-order model is applicable. The IBU-containing composites in higher concentration are characterized with the Korsmeyer-Peppas model, i.e. in this case the erosion and the diffusion determine the release rate of the drug. [3]

## **5. Outlook**

The aim of my doctoral work is to develop and characterize such drug delivery systems which are able to encapsulate water-insoluble or other drug molecules which have weak bioavailability in human body as well as they are suitable for controlled drug release under *in vitro* and *in vivo* circumstances. *In vitro* blood-brain barrier model experiments with the one-layered KYNA-containing core-shell nanocomposites were carried out by the group of Dr. I. Krizbai in the Biological Research Center. Due to increased permeability of the KYNA, J. Toldi et al (Department of Physiology, Anatomy and Neuroscience, University of Szeged) used animal experiments to prove the targeted and efficient drug delivery into the central nervous system by core-shell nanoparticles. As a result of the successful work, a patent, titled “A process for the

*delivery of drug molecules through the blood-brain barrier using core-shell nanocomposites”*  
(File number: P1500356), has been submitted.

## **6. Publication List**

*Identification number in the Hungarian Collection of Scientific Publications (MTMT): 10047822*

### *Publications related to the dissertation*

[1] N. Varga, M. Benkő, D. Sebők, I. Dékány, BSA/polyelectrolyte core-shell nanoparticles for controlled release of encapsulated ibuprofen, *Colloids and Surfaces B: Biointerfaces* 123 (2014) 616–622.

Impact factor: **4,152**

[2] N. Varga, M. Benkő, D. Sebők, G. Bohus, L. Janovák, I. Dékány, Mesoporous silica core-shell composite functionalized with polyelectrolytes for drug delivery, *Microporous and Mesoporous Materials* 213 (2015) 134-141.

IF<sub>2014</sub>: **3,453**

[3] M. Benkő, N. Varga, D. Sebők, G. Bohus and I. Dékány, Bovine serum albumin-sodium alkyl sulfates bioconjugates as drug delivery systems, *Colloids and Surfaces B: Biointerfaces* 130 (2015) 126–132.

IF<sub>2014</sub>: **4,152**

[4] N. Varga, I. Dékány, Structural changes of the BSA protein at various pH and physiological salt solution from Extended to Aged-form, *Int. J. Biol. Macromolec.* (Submitted, IF<sub>2014</sub>: 2,85)

[5] N. Varga, E. Csapó, Z. Majláth, I. Ilisz, I. Krizbai, I. Wilhelm, L. Knapp, J. Toldi, L. Vécsei, Targeting of the kynurenic acid across the blood-brain barrier by core-shell nanoparticles, *Int. J. Pharm.* (Submitted, IF<sub>2014</sub>: 3,65)

Patent related to the dissertation

[6] N. Varga, I. Dékány, L. Knapp, I. Krizbai, Zs. Majláth, J. Toldi, L. Vécsei, *A process for the delivery of drug molecules through the blood-brain barrier using core-shell nanocomposites*, File number: P1500356

**ΣIF =11,757**

Further publication

[7] T. Szabó, Á. Veres, E. Cho, J. Khim, N. Varga, I. Dékány, Photocatalyst separation from aqueous dispersion using graphene oxide/TiO<sub>2</sub> nanocomposites, *Colloids and Surfaces A Physicochemical and Engineering Aspects* 433 (2013) 230–239.

**IF: 2,354**

[8] A. Majzik, V. Hornok, N. Varga, R. Tabajdi, I. Dékány, Functionalized gold nanoparticles for 2-naphthol binding and their fluorescence properties, *Colloids and Surfaces A Physicochemical and Engineering Aspects* 481 (2015) 244-251.

**IF<sub>2014</sub>: 2,752**

[9] V. Hornok, E. Csapó, N. Varga, D. Ungor, D. Sebők, G. Laczkó, I. Dékány, Controlled syntheses and structural characterization of plasmonic and red-emitting gold-lysozyme nanohybrid dispersions, *Colloid and Polymer Science* (2015) DOI:10.1007/s00396-015-3781-7

**IF<sub>2014</sub>: 1,865**

**ΣIF =6,971**

**ΣΣIF =18,728**

Conference presentations

N. Varga, G. Bohus, M. Benkő, I. Dékány, Core-shell nanohybrid particles for controlled release of ibuprofen, Workshop on Functionalized Surfaces and Nanobiocomposites, 26-28.05.2013, Szeged, Hungary (poster)

I. Dékány, N. Varga, M. Benkő, D. Sebők, Mesoporous silica core-shell nanoparticles for controlled release of ibuprofen, 6th International FEZA Conference, 08-11.09.2014. Leipzig, Germany (poster)

N. Varga, M. Benkő, D. Sebők, L. Janovák, I. Dékány, Mag-héj szerkezetű kompozitok előállítása és hatóanyag leadása, Kolloid Munkabizottsági Ülés, 26.09.2014. Eger, Hungary (lecture)

N. Varga, M. Benkő, D. Sebők, I. Dékány, Core-shell nanoparticles for drug delivery, 6th Szeged International Workshop on Advances in Nanoscience, SIWAN6, 15-18.10.2014. Szeged, Hungary (poster)

N. Varga, I. Dékány, A kinurénsav nanokapszulázása és a hatóanyag leadása a véragy-gáton való átjutás modellezése céljából, Kinurenin Kerekasztal, 25.11.2014. Szeged, Hungary (lecture)

I. Dékány, N. Varga, E. Csapó, D. Sebők, Self-assembled 2D and 3D nanoscale materials: core-shell nanoparticles for drug delivery, BIT's 4th Annual World Congress of Nano Science&Technology, 29-31.10.2014., Qingdao, China (lecture)

I. Dékány, N. Varga, E. Csapó, V. Hornok, D. Ungor, Á. Juhász, D. Sebők, Self-assembled core-shell nanoparticles for drug delivery: structural properties and kinetic of the release process, 6th international congress, Bionanomed 2015, 08-10.04.2015. Graz, Austria (lecture)

N. Varga, I. Dékány, Controlled release of encapsulated neurotransmitter from core-shell nanocomposites, 15th European Student Colloid Conference, 08-11.06.2015. Krakow, Poland (poster)

I. Dékány, N. Varga, E. Csapó, D. Sebők, Á. Juhász, L. Janovák, Syntheses and characterization of potential drug carrier nanocomposites, 11th International Conference on Diffusion in Solids and Liquids, 22-26.06.2015. München, Germany (lecture)

I. Dékány, E. Csapó, D. Sebők, N. Varga, Á. Juhász, A fény és a röntgensugarak kölcsönhatása szupramolekuláris rendszerekkel és plazmonikus nanoszerkezetű anyagokkal, MKE2. Nemzeti Konferencia, 08.31-02.09.2015. Hajdúszoboszló, Hungary, (lecture)

N. Varga, I. Dékány, Mag-héj kompozitok fejlesztése célzott és szabályozott hatóanyag leadásra, TÁMOP Tudáspark projekt (TÁMOP-4.2.1.C-14/1/KONV-2015-0013): „A kinurenin program - szabadalmi lehetőségek”, 27.10.2015. Szeged, Hungary (lecture)

N. Varga, I. Dékány, Gyógyszerhatóanyag szállító rendszerek szerkezete és a hatóanyag leadás kinetikája, Kolloid Munkabizottsági Ülés, 06.11.2015. Budapest, Hungary, (lecture)